Inverse analysis on two geotechnical works: a tunnel and a cavern.

S. Eclaircy-Caudron, D. Dias & R. Kastner
LGCIE laboratory, Site Coulomb 3, INSA Lyon, 20 avenue Albert Einstein, 69100 Villeurbanne, France

T. Miranda & A. Gomes Correia
University of Minho, Department of Civil Engineering, Guimarães, Portugal

L. Ribeiro e Sousa
University of Porto, Department of Civil Engineering, Porto, Portugal

ABSTRACT: One of the major difficulties for geotechnical engineers during project phase is to estimate in a reliable way the mechanical parameters values of the adopted constitutive model. In project phase, they can be evaluated by laboratory and in situ tests. But, these tests lead to uncertainties due to the soil reworking and to local character of the test which is not representative of the soil mass. Moreover for in situ tests interpretation difficulties exist due to the non homogeneous character of the strain and stress fields applied to the soil mass. In order to reduce these uncertainties, geotechnical engineers can use inverse analysis processes during construction. This article shows the application of two of these processes (a deterministic and a probabilistic method) on convergence leveling measurements realized during the excavation of the Bois de Peu tunnel (France). Moreover, these two processes are also applied on displacements measured by inclinometers during the excavation of the hydroelectric powerhouse cavern Venda Nova II (Portugal). The two inverse analysis methods are coupled with two geotechnical software (CESAR-LCPC and FLAC^{3D}) to identify soil parameters. Numerical and experimental results are compared.

1 INTRODUCTION

The purpose of an inverse analysis process is the identification of parameters using tests results or/and experimental measurement carried out during works. Various methods exist. Hicher (2002) distinguishes three kinds: analytical methods, correlation and optimization methods. Optimization methods are applied when model parameters are not appropriate to be used in a direct approach by graphic construction or in an analytical approach. By this method, the inverse problem is solved using an algorithm which minimizes a function depending on all parameters. This function is generally called “cost function” and corresponds to the difference between numerical and experimental measurements. The experimental results can come from various origins: laboratory tests, in situ tests or work measurement data. Two types of optimization methods are distinguished: deterministic and probabilistic methods. The deterministic methods include gradient, Newton, Gauss-Newton or Liebenberg Marquardt optimization algorithms. Several researches aiming at parameter identifications based on deterministic methods were carried out in the last years. Zentar (2001) tried to identify some mechanical parameters of the Saint-Herblain clay using the results of pressuremeter tests and the optimization software SiDoLo (Pilvin 1983). He considered an elastoplastic model with or without hardening. In spite of the identification methods development, a few of them were applied to real cases like tunnels or deep excavations (Jeon et al. 2004, Finno et al. 2005).

The deterministic methods present some advantages. The iteration number required to achieve the optimization process is relatively low. But, if the cost function presents several local minima, the deterministic methods can converge towards the first found minimum. This major drawback explains why these methods are seldom used for complex problems. For such problems probabilistic methods are preferred. Probabilistic methods include evolutionary algorithms

such as genetic algorithms and evolution strategies. Evolutionary algorithms reproduce the natural evolution of the species in biological systems and they can be used as a robust global optimization tool. The major principles of genetic algorithms were developed by Goldberg (1991) and renders (1995). Evolution strategies (Schwefel, 1985) start searching from an initial population (a set of points) and transition rules between generations are deterministic. The search of new points is based on mutation and recombination operators. Recent researches applying genetic algorithms to soil parameters identification for a constitutive model have been undertaken in geotechnic (Levasseur et al. 2005, Samarajiva et al. 2005). Evolution strategies were also recently applied to problems in many domains (Costa et al. 2001).

First, this paper presents briefly the used optimization software, SiDoLo and the used evolutionary algorithm. Then the numerical modeling of the two geotechnical works and the followed approach are detailed. Finally, results obtained by the two processes are compared and influence of some data in the evolutionary algorithm is highlighted.

2 PRESENTATION OF THE OPTIMIZATION METHOD USED

2.1 *The optimization software, SiDoLo*

SiDoLo is coupled with the geotechnical software CESAR-LCPC (Itech 2002) or FLAC^{3D} (Itasca 2005). The coupling principle is illustrated in figure 1.

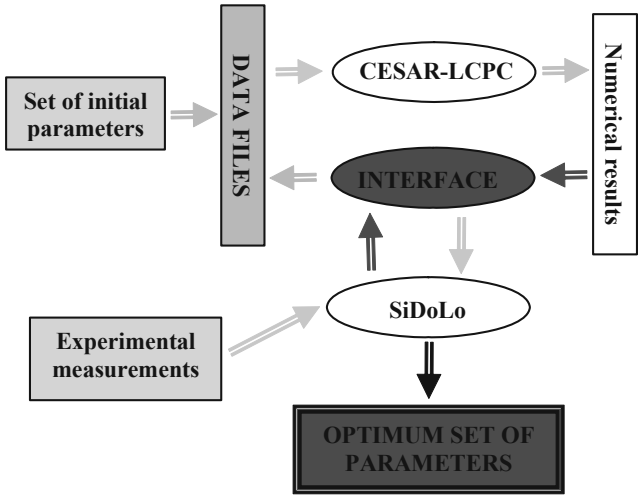

Figure 1. Principle of the coupling

Through this coupling, SiDoLo compares numerical results with experimental measurements, in order to calculate the cost function. When the cost function is lower than a fixed value, then the optimization process stops. The cost function L(A) is expressed by the following finite sum:

$$L(A) = \sum_{n=1}^{N} \frac{1}{M_n} \sum_{i=1}^{M_n} {}^{T}[Z_s(A,t_i) - Z_s^*(t_i)].D_n.[Z_s(A,t_i) - Z_s^*(t_i)] \tag{1}$$

where A are the model parameters, N is the number of experimental measurements; $[Z_s(A,t_i)-Z_s^*(t_i)]$ is the difference between numerical and experimental results evaluated only at Mn observation steps t_i and D_n is the weighting matrix of the n^{th} test. Measurements accuracy can be taken into account by weighting coefficients.

SiDoLo uses a hybrid optimization algorithm, which combines two typical minimization methods: the gradient method and a variant of the Lavenberg-Marquardt method to accelerate the convergence when the solution is close. More details on the SiDoLo approach can be found in Eclaircy-Caudron et al. (2006).

2.2 *The algorithm based on evolution strategies*

The algorithm used was developed by Costa et al. (2001). This algorithm was adapted to the problems studied in this paper, and as for SiDoLo, requires creating an interface with computer codes. The population entities are vectors of real coded decision variables that are potential optimal solutions. An initial population is generated and then each following generation, λ offspring are generated from μ progenitors by mutation and recombination. Then the best entities are selected for next generation among the μ+λ members according to their cost function value. Finally, the μ best of all the μ+λ members become the parents of the next generations. Important features of evolution strategies are the self adaptation of step sizes for mutation during the search and the recombination of entities that is performed between ρ individuals. This algorithm, named generally (μ/ ρ+λ) algorithm, is illustrated in figure 2.

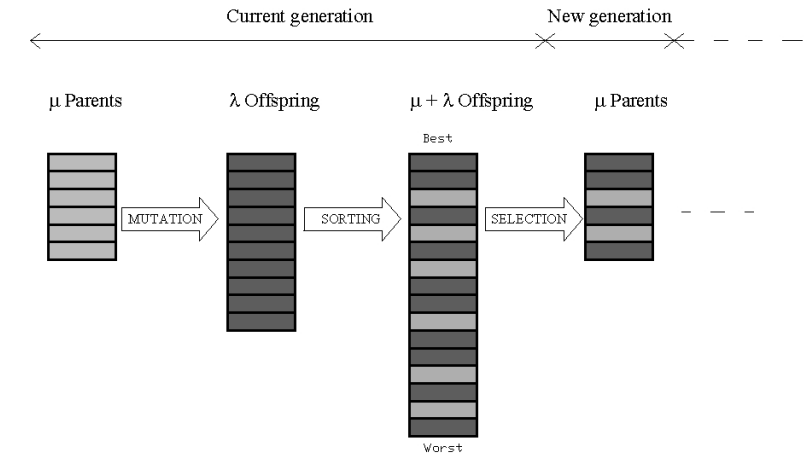

Figure 2. Principle of the (μ/ ρ+λ) evolution strategies (Costa et al., 2001)

The algorithm stops when one of the following conditions is verified:

- The maximum number of generations is reached
- The difference between the two extreme values of the cost functions is lower than 10^{-5}
- This difference divided by the average of the cost functions values is lower than 10^{-5}

Various error functions are considered. First, the same function than in SiDoLo is introduced in the algorithm. Then, the following error function is considered.

$$L_E(A) = \sqrt{\frac{1}{N}\sum_{i=1}^{N}\frac{[Z_s(A,t_i) - Z_s^*(t_i)]^2}{[\varepsilon + \alpha . Z_s^*(t_i)]^2}} \tag{2}$$

The ε and α variables represent respectively the absolute and relative error of measurements. Different values of these two variables are tested.

3 THE FOLLOWED APPROACH

3.1 *Case 1: Application to the Bois de Peu tunnel*

3.1.1 *Presentation of the tunnel*

The Bois de Peu tunnel is situated near Besançon in France. It is composed of two tubes. The excavation length is about 520 meters per tube for a cover height which varies between 8 meters and 140 meters. Four kinds of supports were foreseen in the project phase for four materials types: limestones, marls, interbeding of marls and limestones and clays. The studied section is located near one of the two tunnel portals where interbeding of marls and limestones were expected. A face levelling of this section is showed in figure 3. The lining support set up in this area is composed of a mixed tunnel support by shotcrete with a thickness of 0.2 m and steel ribs.

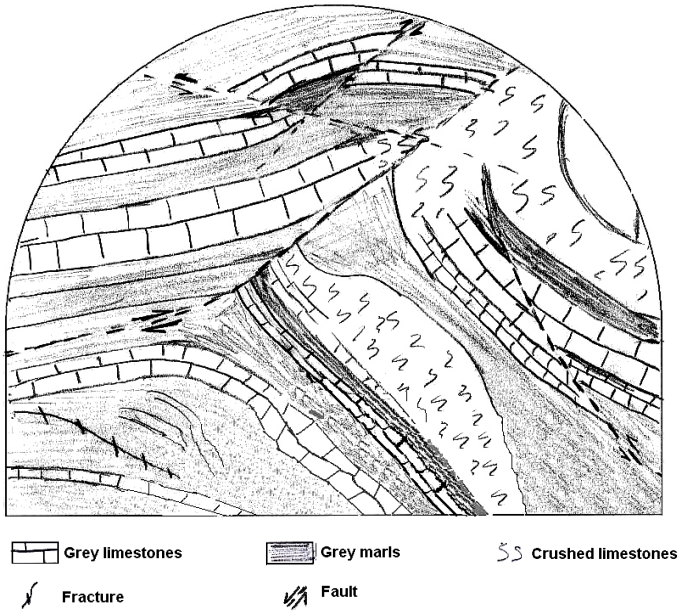

Figure 3. Face leveling

The tunnel is dug with a constant step of 1.5 m. The cover height is equal to twenty six meters. From the site investigations, two kinds of design characteristics were defined: probable and exceptional. They are resumed in table 1.

Table 1. Design characteristics

Parameters	γ kN/m3	E MPa	C MPa	φ °	ν -
Probable	24.8	1600	0.70	40	0.3
Exceptional	24.0	750	0.21	36	0.3

3.1.2 *Numerical model*

Due to time consuming of three dimensional calculations, tunnel excavations are often taken into account by two dimensional modelling. We adopted a transverse plane strain model, taking into account the real geometry, the excavation and tunnel support being modelled by an unconfinement ratio (Panet, 1995). Only a half section is represented due to symmetry. The grid extents are 75 m (=6D) in all directions in order to avoid the influence of the boundaries. The grid (figure 4) contains around 3900 nodes and 1850 elements with quadratic interpolation (six nodes triangles and 8 nodes quadrangles). The initial stress field is anisotropic. An earth pressure ratio of 0.7 is adopted. This value was obtained from in situ tests. Steel ribs and sprayed concrete are simulated by a homogeneous support with equivalent characteristics. This support is assumed to have a linear elastic behaviour. A linear elastic perfectly plastic model with a Mohr Coulomb failure criterion and non associate flow rule is considered to represent the soil mass.

Three computing phases are defined. First the initial stress field is applied. After, the tunnel is excavated. In this phase, the unconfinement ratio at the time of the support installation is applied. Finally the homogeneous support with 0.24 m width is activated. A total unconfinement is applied.

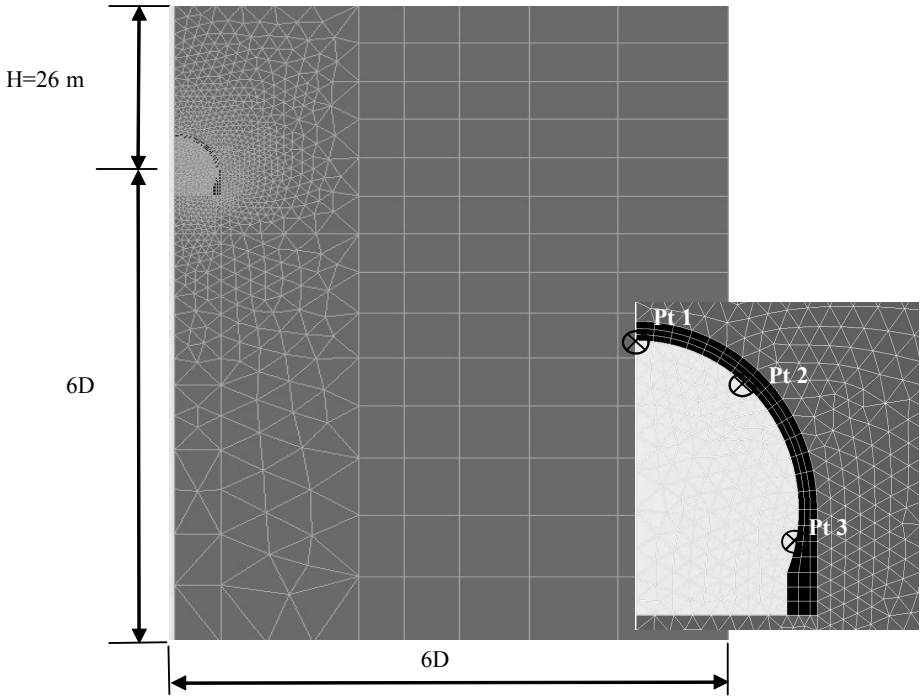

Figure 4. The grid and its dimensions

3.1.3 *Experimental results*

Figures 4 and 5 locate the three experimental measurements points used for optimization. Five measurements are observed for these three points: levelling for these three points and horizontal displacements for the points 2 and 3. They correspond to convergence and levelling measurements of the tunnel wall in a given cross section (point 1 to 3 in figures 4 and 5).

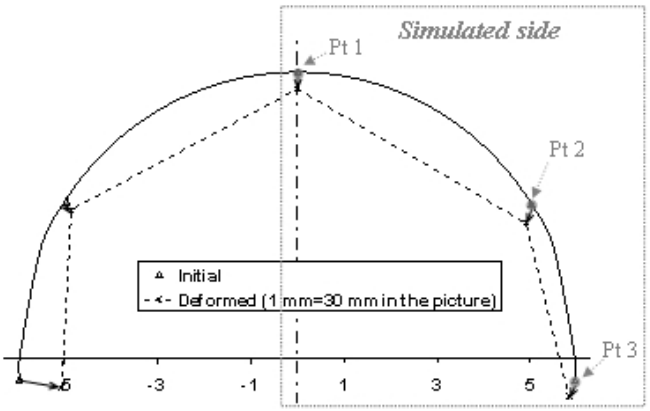

Figure 5. The observations points and deformed section

The convergence and levelling measurements of this section are reported in figures 6 and 7. These measurements permit to deduce the horizontal and vertical displacements of each point. The convergence is maximal for wires 4 and 5. It reaches 30 mm for wire 4. Moreover leveling is more important for targets 3, 4 and 5 than for the others. It reaches 13 mm. So, these measurements showed a dissymmetrical deformation of the section. In optimization process average displacements measured at equilibrium are used. The dissymmetry is confirmed by the section deformation presented in figure 5 where the crown displacement is assumed purely vertical. The experimental results considered in the optimization process correspond to the average displacements observed at the two sides.

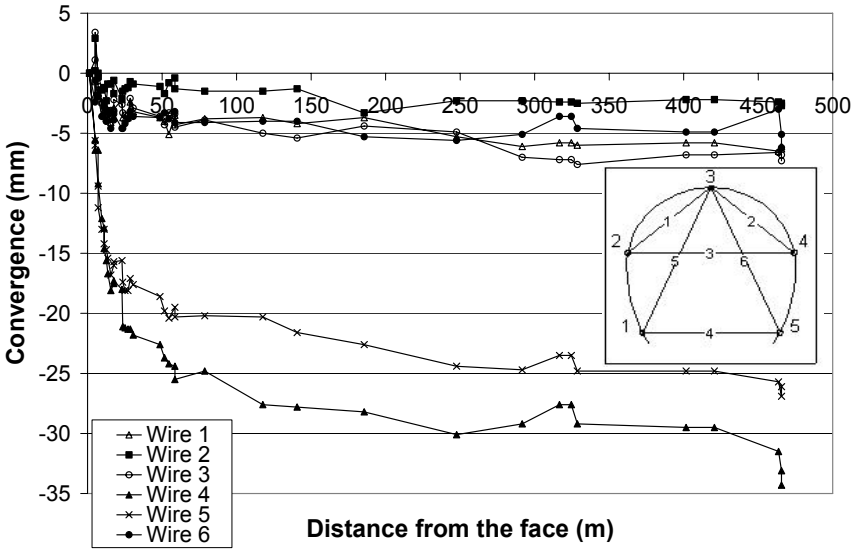

Figure 6. Convergence measurements

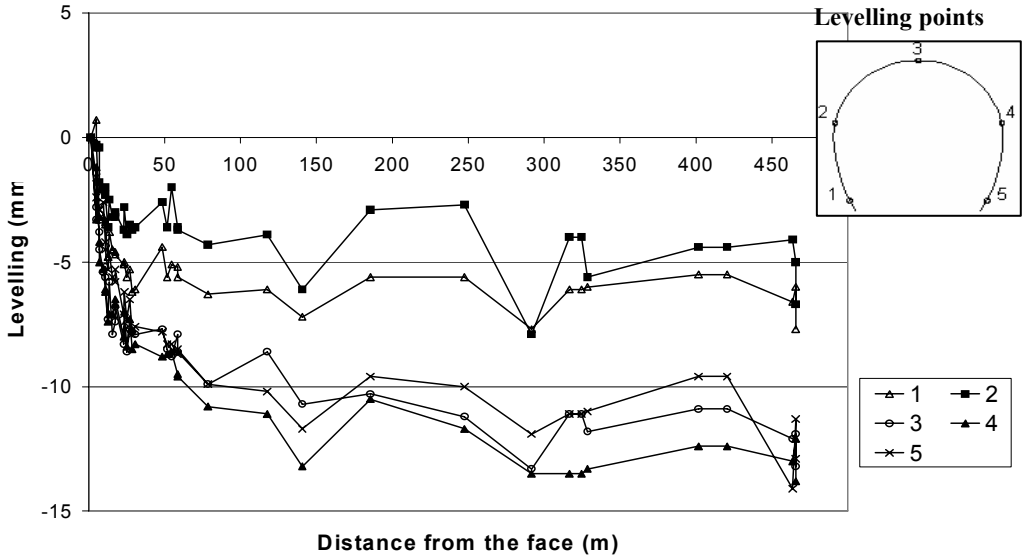

Figure 7. Levelling measurements

3.1.4 *Unknown parameters*

In plane strain calculation, the introduced unconfinement ratio λ at the time of support installation might be calculated by the convergence-confinement method (Panet, 1995) if the constitutive model parameters were well known. But in this study, it is considered as an additional parameter to identify. Before using inverse analysis, a sensibility study was performed. The Poisson ratio and the dilatancy angle are parameters which have low influence on the observed variables. So, these parameters could not be identified with these measurements. Only parameters λ, C, E and φ, might be evaluated.

Validation studies (Eclaircy-Caudron et al. 2006) were performed with SiDoLo on this numerical model in order to define which parameters might be identified according to the available experimental measurements. These studies showed that with convergence and levelling measurements no more than two parameters could be identified. But SiDoLo always succeeded to identify φ and λ even if they were unknown because they have more influence on the convergence and levelling measurements than the others. In order to verify the provided solution an evolution strategies algorithm is used in complement of the software SiDoLo.

3.2 *Case 2: Application to the Venda Nova II hydroelectric powerhouse cavern*

3.2.1 *Presentation of the powerhouse cavern*

The Venda Nova II powerhouse cavern is located in the North of Portugal, about 55 km of the town Braga. The powerhouse complex includes two caverns interconnected by two galleries. The caverns have respectively the dimensions as follows: 19.00 m × 60.50 m and 14.10 m × 39.80 m. Their axes are spaced by 45.00 m. They are situated at a 350 m depth. Both caverns have vertical walls and arch roofs. The roof of both caverns is situated at different levels. Moreover, the main cavern has various floors while the other has a single floor. The geometry is illustrated in figure 8. The powerhouse complex is situated in a rock mass characterized by medium-size grain granite of a porphyritic trend with quartz and/or pegmatitic veins and beds, which are, sometimes, rose. The rock mass also includes embedment of fairly quartzitic micaschist. In order to investigate the geotechnical characteristics of the rock mass in depth, four deep and subvertical boreholes were performed. Laboratory tests were done on rock samples resulting from boreholes. These tests permitted to identify three geological and geotechnical zones. The zone where the caverns are located presents a Young modulus of 54 GPa and a Poisson ratio of 0.17. Moreover, in situ tests are carried out before the beginning of the main work and after completing the access tunnel to the powerhouse. In fact, an exploration gallery was excavated from the top of the access tunnel and parallel to the caverns axis. In situ tests confirm the presence of four main families of discontinuities and led to values ranging from 33 to 40 GPA for the deformability modulus. The in situ stress state of the rock mass was also characterized. The vertical and horizontal stresses aligned with the longitudinal axes of the caverns correspond to the earth weight. The horizontal stress normal to the longitudinal axes of the caverns is 2 to 3 times higher than the other stresses.

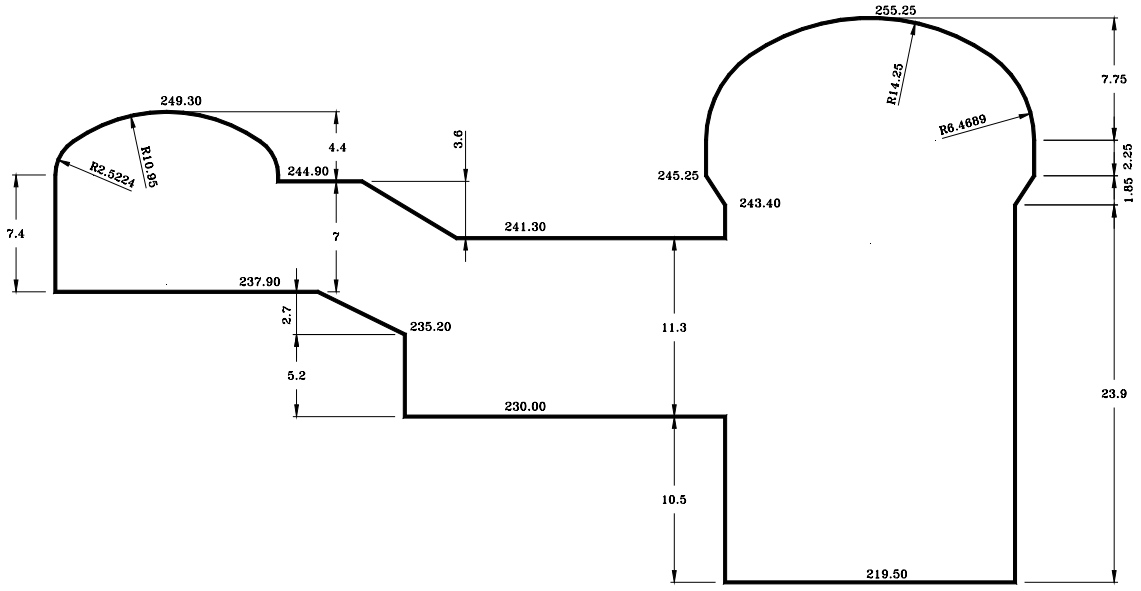

Figure 8. The powerhouse cavern geometry

3.2.2 *Numerical model*

– The caverns excavation was modelled in 3D with the finite difference computer code FLAC^{3D} in order to simulate the real complex geometry of them and the excavation stages. Figure 9 shows the mesh performed with the hexahedral-Meshing Pre-processor, 3DShop. The grid dimensions are 300 m in the transversal direction, 460 m in the longitudinal direction and its height is 275 m. A layer of 75 m is modelled under the caverns. A cover height of 350 m is simulated. The mesh contains around 47000 grid-points, 44000 zones and 1100 structural elements. The simulated excavation stages are lightly different from the real stages but the rock mass staying in elasticity, final displacements are the same. Figure 10 shows the excavation sequences modelled.

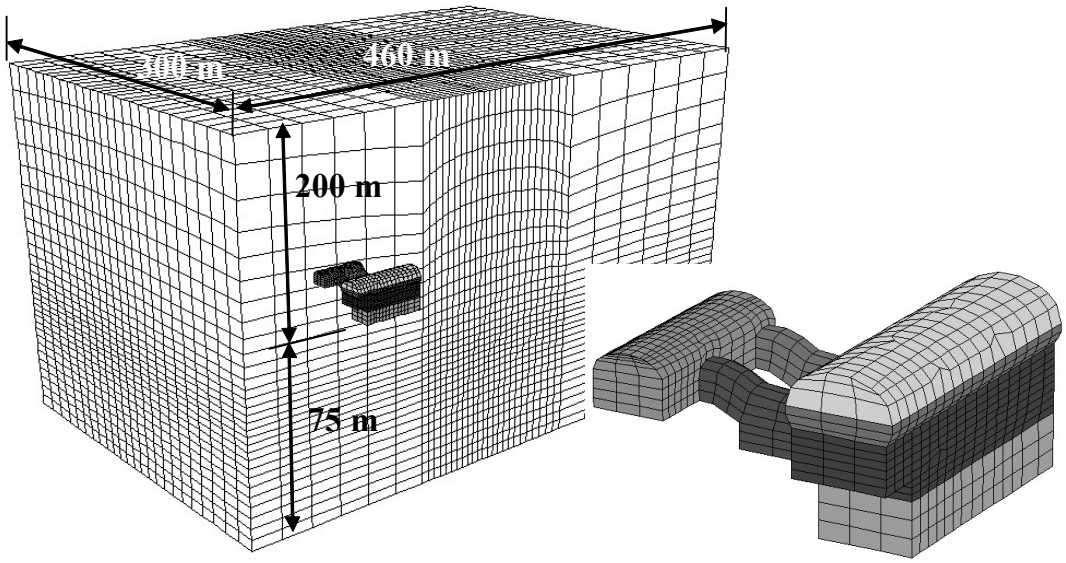

Figure 9. The 3D mesh.

Stage 1	Stage 2	Stage 3
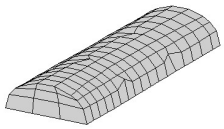	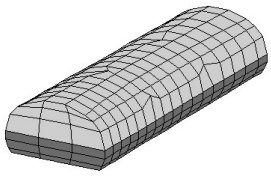	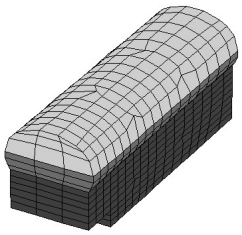
Stage 4	Stage 5	Stage 6
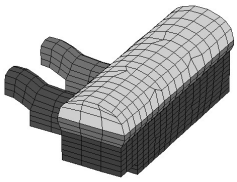	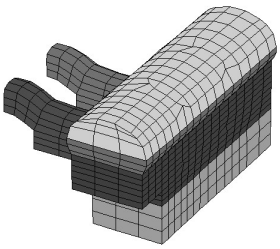	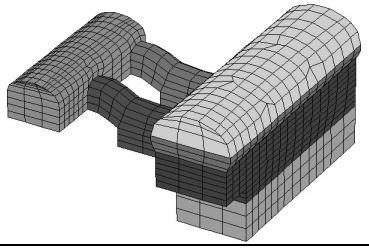

Figure 10. The excavation stages.

The excavation steps are the following:
- 1: Total excavation of the main cavern arch. Set up of fibre sprayed concrete (thickness: 25 cm) on the arch.
- 2: Excavation of the main cavern arch until 1.5 m below the base level of the support beams of the rail tracks and set up of fibre sprayed concrete on the walls cavern (thickness: 25 cm).
- 3: Excavation of the main cavern until the level of the interconnecting galleries.
- 4: Excavation of the interconnecting galleries and set up of fibre sprayed concrete on the galleries arch (thickness: 25 cm).
- 5: Achievement of the main cavern excavation

6: Excavation of the transformer cavern and set up of fibre sprayed concrete (thickness: 25 cm) on the arch

In the numerical modelling, an elastic perfectly plastic constitutive model with a Mohr Coulomb failure criterion is assumed to represent the rock behaviour. The sprayed concrete is simulated by shell elements with a linear elastic and isotropic constitutive model, with a Young modulus of 15 GPa and a Poisson ratio of 0.2. The rock bolts are simulated by cable elements, with two nodes and one axial free degree. These elements can yield a tensile stress.

3.2.3 *Experimental results*

A monitoring program was established in order to evaluate the behaviour of the rock mass and the support system and to observe displacements in the rock during and after construction. Convergence targets were installed in several sections. Besides the convergence measurements, 11 extensometers were installed in two sections along the caverns axis (figure 11). In the powerhouse cavern extensometers were installed in two sections, while only one in the other cavern was installed. Almost all the extensometers are double. Just the ones installed in the wall on the main caver are triple and of larger length (EF1 and EF5 in Figure 11). Figure 12 shows the evolution of displacements in extensometers 1 and 5. Figure 13 gives the displacement value measured at the last stage for each extensometer.

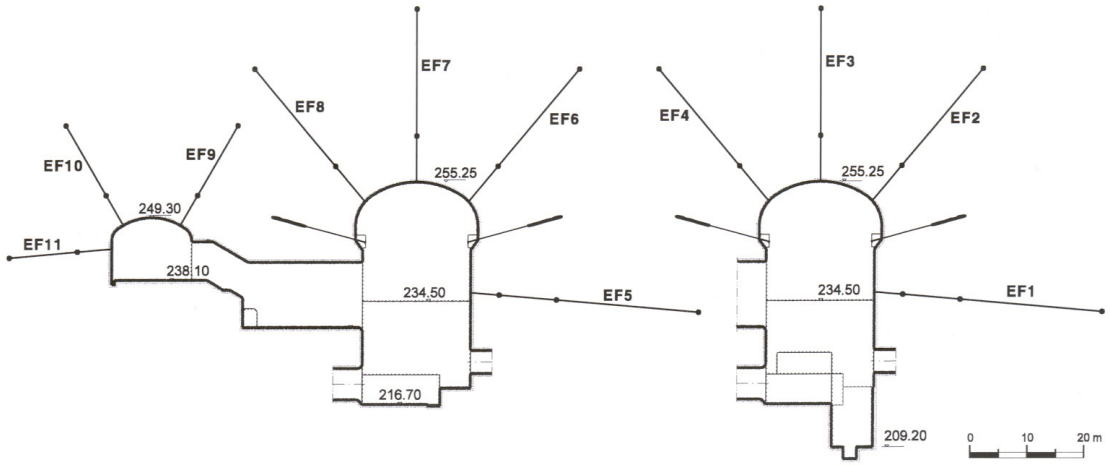

Figure 11. Location of the extensometers in the two cross sections

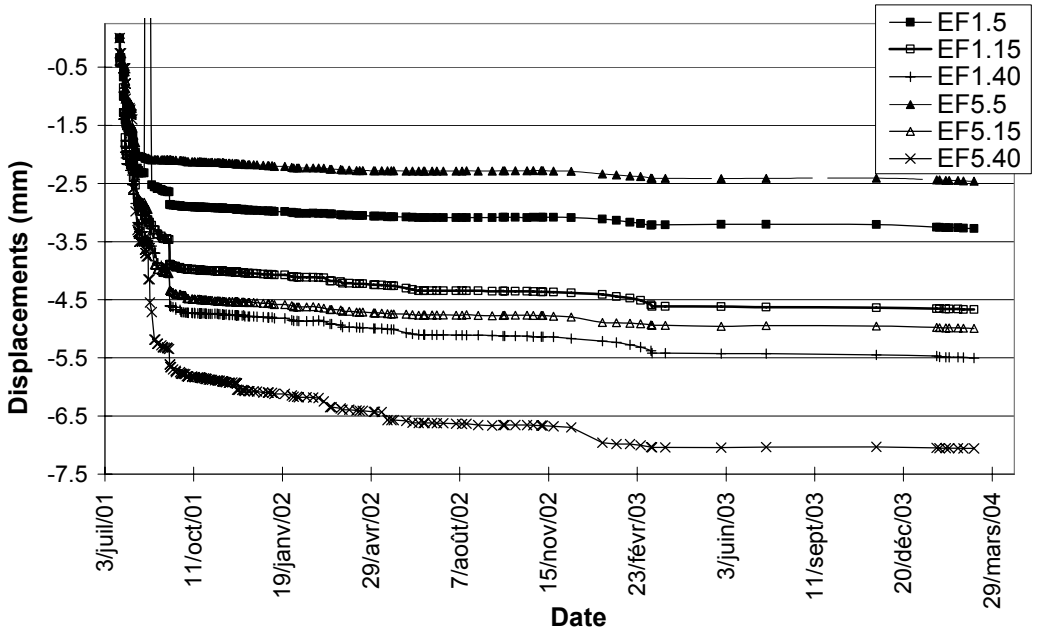

Figure 12. Evolution of the measured displacement in extensometers 1 and 5

In optimization process, displacements measured at the last excavation stage are used. In validation study, all extensometers are considered. So, 24 displacements are available in the optimization process. In the case of the application on the in situ measurements, only 20 displacements are used in the optimization process because some values are not considered due to measurement errors (EF 3.8, 3.3, 4.8 and 4.3).

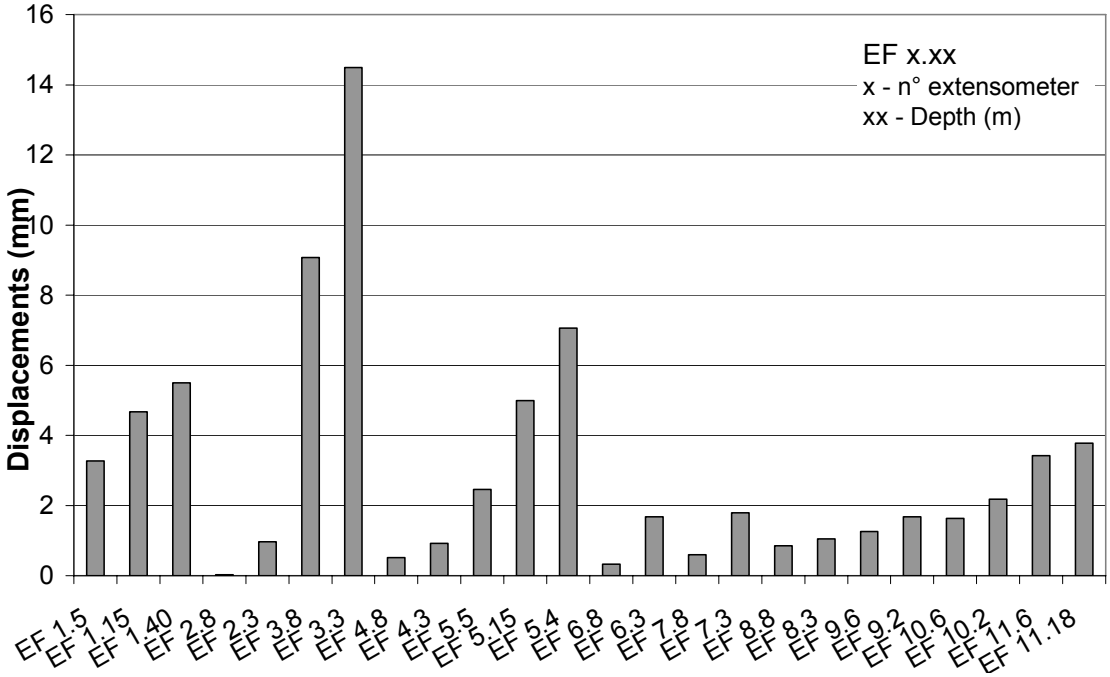

Figure 13. Displacements value measured in each extensometer at the last excavation stage.

3.2.4 *Unknown parameters*

Previously studies permitted to obtain mechanical properties of the rock by using Artificial Intelligence techniques (Miranda et al. 2005). These are the following: 45 GPa for E, 54° for φ and 4 MPa for C. Due to the good strength of the rock, a few plastic zones appear. So the value of the two parameters C and φ has low influence on the numerical results. A value of 0.2 is adopted for the Poisson ratio and the dilatancy angle is taken equal to 0°. These two parameters have also low influence on the numerical result. Then, only the Young Modulus might be identified by inverse analysis. Besides, many uncertainties reside on the in situ stresses ratio value R. So, as this parameter influences the numerical results, it might be also identified by inverses analysis.

Validation studies were performed with the two optimization processes on this numerical model. These studies show that it is possible to identify the Young modulus and the in situ stresses ratio just from the displacements measured by extensometers. So, this paper presents the identification results performed on these two parameters and compares the results provided between the two processes.

4 RESULTS

4.1 *Case 1:Bois de Peu tunnel (France)*

4.1.1 *Comparisons between the two methods*

Several identification attempts were performed with SiDoLo, confirming that SiDoLo provides approximately the same values of φ and λ in all cases. They also showed that the friction angle was lower than the project value (between 10 and 20°).

One example of identification is presented here, where three vertical and two horizontal displacements are used in the optimization process. For each identification several initial values (referred as a, b and c) of the unknown parameters are tested in order to show the influence of the initial value. Only the Young modulus E and the cohesion C are identified. λ and φ are fixed respectively to the average of values provided by identifications of the four parameters (E, C, φ, λ). A friction angle of 14° and an unconfinement ratio of 0.7 are adopted. The enabled ranges in SiDoLo are resumed in table 2. Table 2 gives also the obtained values. Several solutions are found by the optimization process according to the introduced initial values. SiDoLo does not succeed to find the best couple. It provides local minima. Displacements computed after optimization are showed in figure 14.

Table 2. The identification results realized with SiDoLo

Set	E MPa	C MPa
Range	100-2000	0.10-1
a	217	0.13
b	100	0.19
c	102	0.19

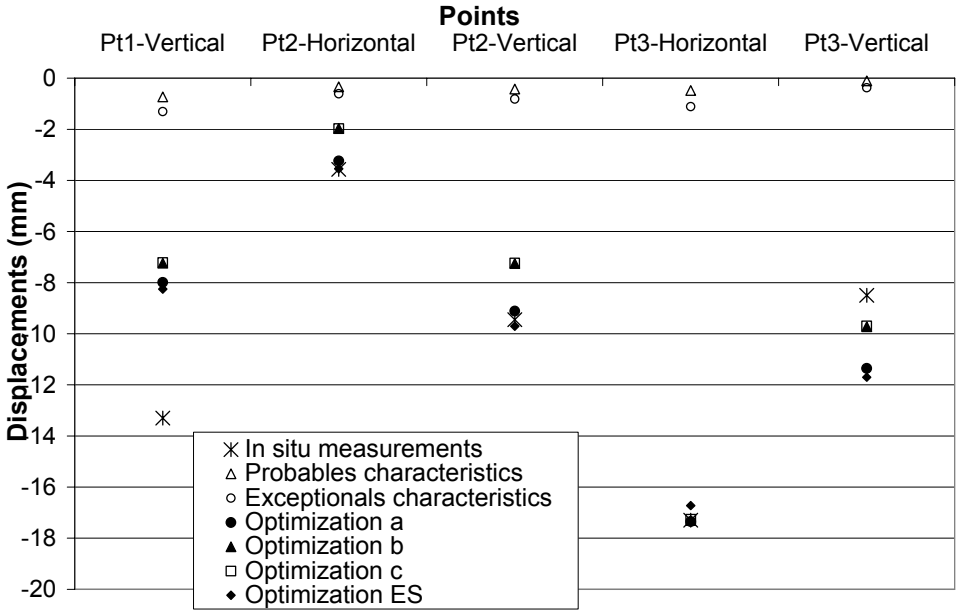

Figure 14. Comparisons between the measured and computed displacements after optimization by SiDoLo

For points 2 and 3 numerical results are close to the measured displacements. The vertical displacements computed at point 1 are lower than the one measured. The vertical displacement measured at the tunnel crown appears difficult to reproduce in the numerical model. Although the face leveling showed in figure 3 highlights a disturbed geology with folds and faults, an homogeneous medium is considered in the model. A more complex model seems to be required to simulate the real behavior of the tunnel crown.

In order to avoid local minima, the evolution strategies algorithm is used. The same identification is realized. This identification allows verifying the solutions found by SiDoLo. The same ranges are enabled for parameters. The number of generations is limited to 50 in order to keep acceptable computation times. The parent and recombination population size are 10 and the offspring population size is 20. The evolution strategies algorithm stopped when the maximum number of generations is reached, the cost function being still relatively important and the stop criteria on this function cannot be reached. The design characteristics, the best member provided by the Evolution Strategies algorithm (ES) and solutions provided by SiDoLo are resumed in table 3.

Table 3. Design characteristics and optimized values.

Parameters	E MPa	C MPa	φ °	λ -
Probable	1600	0.7	40	-
Exceptional	750	0.21	36	-
SiDoLo	100-217	0.13-0.19	14*	0.7*
ES	242.7	0.12	14*	0.7*

* Fixed values

Figure 15 presents the evolution of the cost function. The cost function is not convex and shows a valley. A decrease of parameter E is counterbalanced by an increase of C in a small variation domain. So it is difficult to identify these two parameters with only convergence and leveling measurements. Moreover the value of the cost function is important, confirming that the numerical model should be improved. Figure 15 shows also the parents at initial and final generations. At initial generation parents are dispersed in all research space. At later generation they are located in the valley and are close to each other.

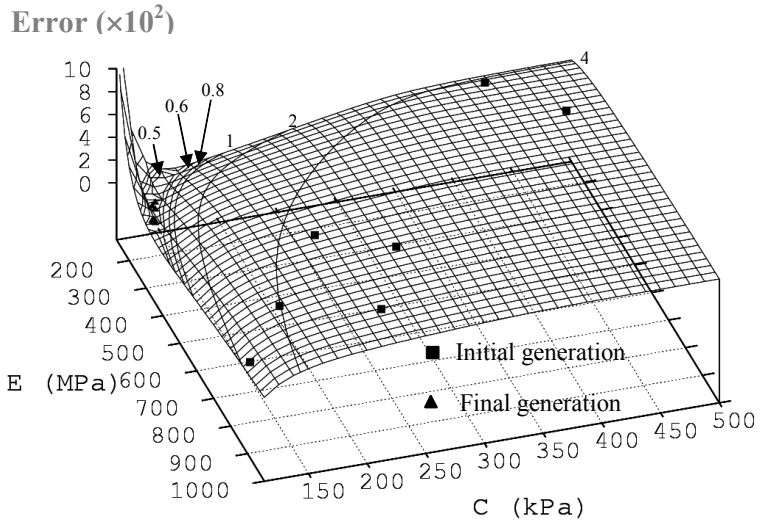

Figure 15. Evolution of the cost function and representation of initial and final generation's parents

Figure 16 locates the three couples found by SiDoLo and the best member found by the evolution strategies algorithm after identification. The error function value is also reported. Solutions found by SiDoLo are situated in the valley and correspond to local minima. The evolution strategies algorithm provides a global minimum.

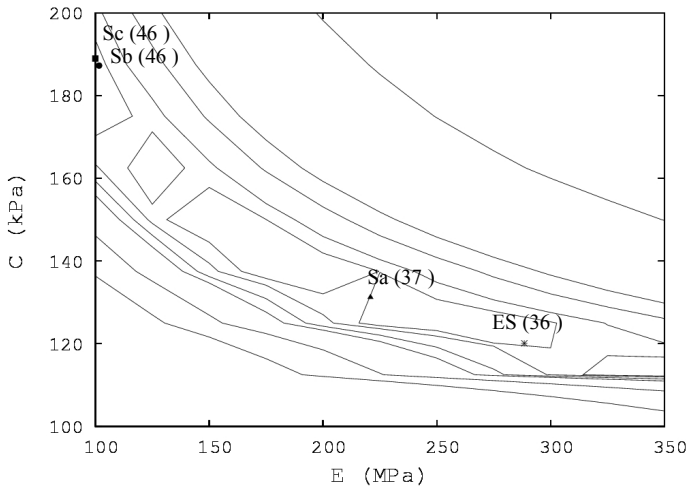

Figure 16. Location of the solutions found by SiDoLo (Sa, Sb and Sc) and the best member found by the evolution strategies algorithm (ES).

4.1.2 *Influence of the error function*

The two error functions presented in equations 1 and 2 are compared. For the second error function, different values of ε and α are tested. All the error functions tested present a valley but the valley extend depends on the error function and on the ε and α values. Figure 17 showed the evolution following E of the different cost functions for a fixed value of C close to the global minimum. The error value reported in figure 17 is not the real value. It corresponds to the real

value minus the minimum value in order to set all curves at the origin. The minimum error is reported on each curve. In this figure the different valleys are visible. For an absolute value of 1 mm and a relative value of 0 the valley is more condensed than for the others. So it is easier to find the global minimum with this error function. The algorithm convergence is similar for all the error function.

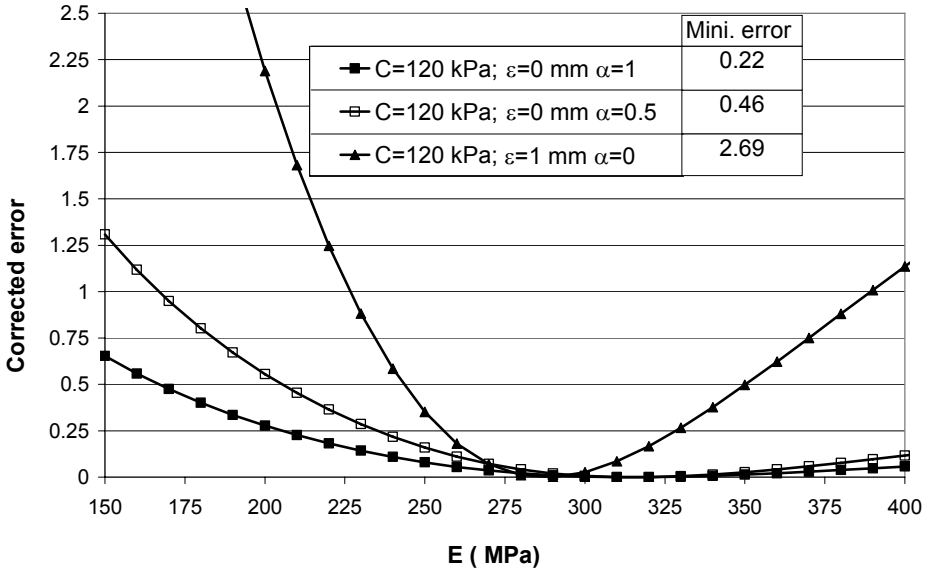

Figure 17. Evolution of the $L_E(A)$ error function for several couples of parameters (ε, α) following the Young modulus for a fixed cohesion value and their minimum value

The solution found by the evolutionary algorithm varies according to the values of absolute and relative errors. Table 4 resumes the found solutions and the computation time. The computation time with SiDoLo is also given. The same solution is found if just a relative error or an absolute error is considered but this solution changes according to the considered type of error. The calculation time is similar for all the error function. But it is very important compared to the computation time required by SiDoLo.

Table 4. Found solutions according to the error function and calculation time

Error	E MPa	C MPa	Error	Time Hours
ε=0 ; α=1	332	0.118	0.22	56
ε=0 ; α=0.5	332	0.118	0.46	55
ε=1 mm ; α=0	289	0.12	2.69	53
SiDoLo	100-217	0.13-0.19	37-46	1,5

4.1.3 *Influence of the population size*

Table 5 gives the solutions provided by the algorithm and the calculation time in two cases. In the first case a parent and recombination population size equal to 10 and a offspring population size of 20 is adopted. In the second case, values of 15 and 30 are respectively adopted for these population sizes.

Table 5. Found solutions according to the population size and calculation time

Cases	E MPa	C MPa	Error	Time Hours
Case 1	288	0.120	2,69	53
Case 2	252	0.125	2.69	84
Difference	12 %	4 %	0 %	50 %

For each calculation, the stop criteria (10^{-5}) cannot be reached; then it is the fixed maximum number of generations which stopped the calculation. For the second case the time is greater about 50 %. With a difference of 12 % on the Young modulus and 4 % on the cohesion, these two calculations give the same error function value. So, due to the computation, it does not seem necessary to increase the population size in our studied case.

4.2 *Case 2: hydroelectric powerhouse cavern (Portugal)*

4.2.1 *Identifications with SiDoLo*

The initial values introduced in SiDoLo are the following: 45 GPa for E and 2 for the in situ stress ratio R. First, the twentieth values of displacements are considered in the optimization process. Figure 18 compares the measured displacement to the computed displacements with the initial values and with the optimized values of the two parameters. It also gives the respective error function values. Displacements computed with the optimized values are closer to the experimental measurements than those computed with initial values excluded for 1.5, 1.15, 5.5, 5.15, 9.2, 10 and 11 (so for 9 observations points). Despite of that, the error function computed with the optimised value is lower than with initial values. So, the using of the optimization software SiDoLo permits to improve the fitting of the numerical values on experimental values. Extensometer 1 and 5 are the same location in the two main cavern cross sections. Extensometers 9, 10 and 11 are located in the small cavern. It could be interesting to do identification only on the main cavern monitoring and in two steps: first, on the monitoring of the first cross section (EF 1 to 4) and after on the other section (EF 5 to 8).

The difference $[Z_s(A,t_i)- Z_s^*(t_i)]$ between the computed value $Z_s(A,t_i)$ and the experimental value $Z_s^*(t_i)$ is always of the same sign excluded for values EF 1.15 and EF 5.4. In fact, for these observations points, the computed value before optimization is more important than the measured values while after optimization, this value is lower than the measurement. In a second time, these two displacements will not be considered in the optimization process. So, only 18 displacements will be used for the identification.

Figure 19 shows the error function value for each displacement and in the two cases: before and after optimization. With initial values, maximal error functions are obtained for EF 1.4 and 2.3 while they are obtained for EF 1.5 and 11.6 with optimized values.

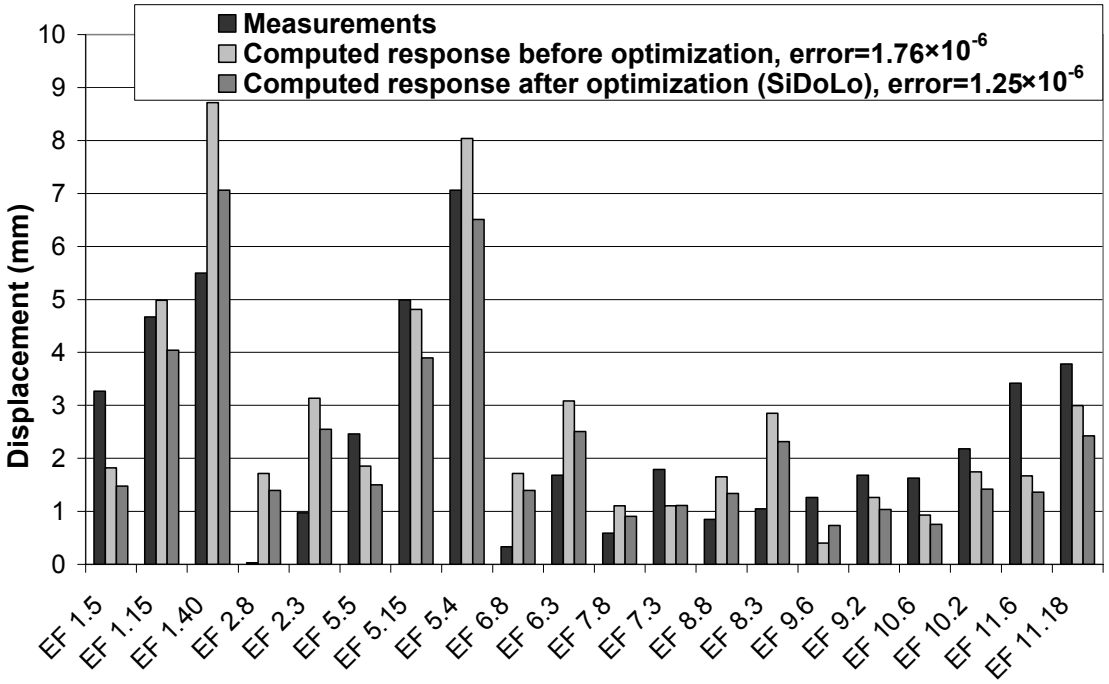

Figure 18. Comparisons between experimental and numerical measurements after the first identification attempt with SiDoLo.

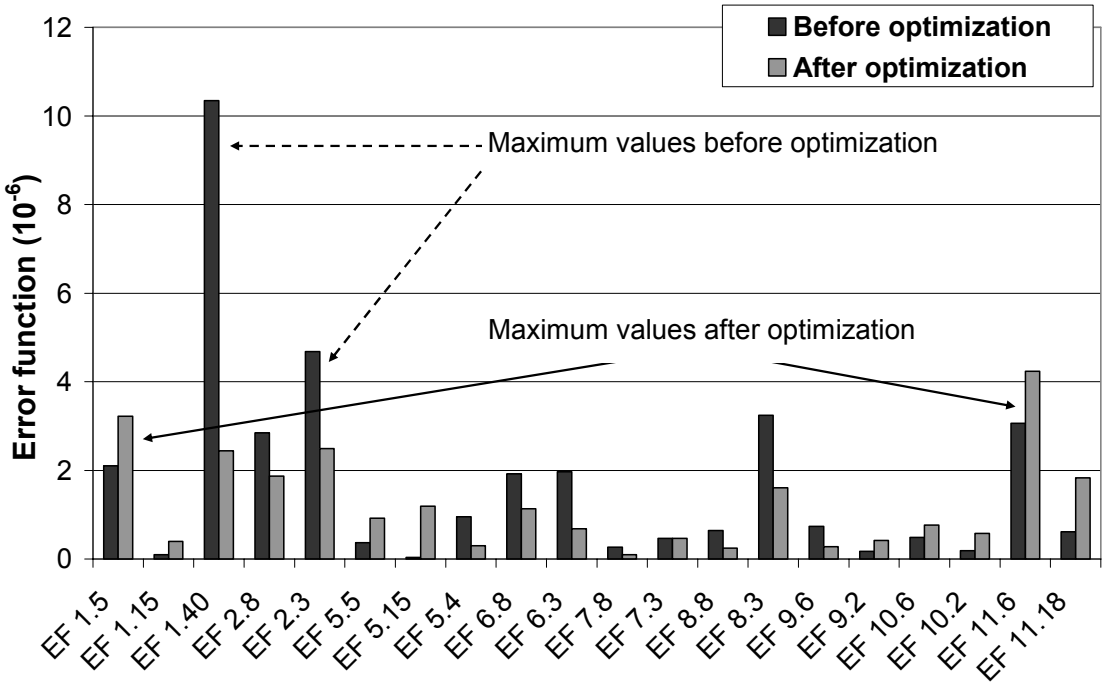

Figure 19. The error function values during the first identification attempt with SiDoLo

In a second time, identifications are performed only on 18 displacements. Table 6 resumes the parameters values provided by SiDoLo at the end of the two identification attempts, the respective error function and the iteration number required to achieve the identification process. For the second attempt the iteration number is not so important than for the first attempt. But, the error function is more important than for the first identification attempt. So, the fitting of the numerical values on experimental values is not improved.

Table 6. Results of the two identification attempts with SiDoLo

Cases	E GPa	R -	Error function $\times 10^{-6}$	iteration	Time Hour
Initial values	45.0	2	1.76 or 1.7	-	-
Attempt 1	55.0	1.98	1.25	25	27
Attempt 2	56.7	1.90	1.34	12	14
Difference	3 %	-4.2 %	7.2 %	-108 %	-93 %

Figure 20 compares the measured displacement to the computed displacements with the initial values and with the optimized values of the two parameters. It also gives the respective error function values. Similar observations to those obtained for the first identification attempt can be made. The error function computed with the optimised value is lower than with initial values. The difference $[Z_s(A,t_i)- Z_s^*(t_i)]$ between the computed value $Z_s(A,t_i)$ and the experimental value $Z_s^*(t_i)$ is always of the same sign.

A similar error function value for each displacement to the one computed in the first identification attempt is obtained.

Figure 21 shows the plastic zones computed at the last excavation stage with the optimized values obtained for the second identification attempt (E=56.7 GPa and R=1.9). Plastic zones are very limited with the two optimized parameters sets. So, it could be very difficult to identify C and φ. These parameters have no influence on the results. Maybe, it might be interesting to adopt an elastic linear constitutive model to represent the rock behaviour and to compare the computed displacements. Besides, the computation time will be shorter.

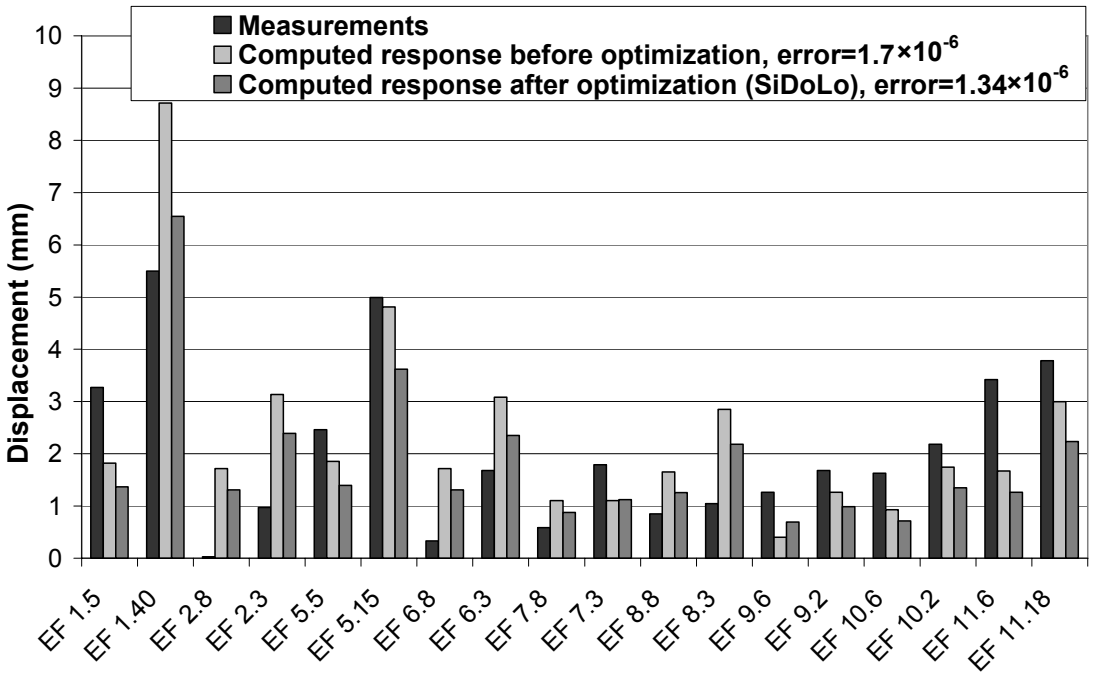

Figure 20. Comparisons between experimental and numerical measurements after the second identification attempt with SiDoLo.

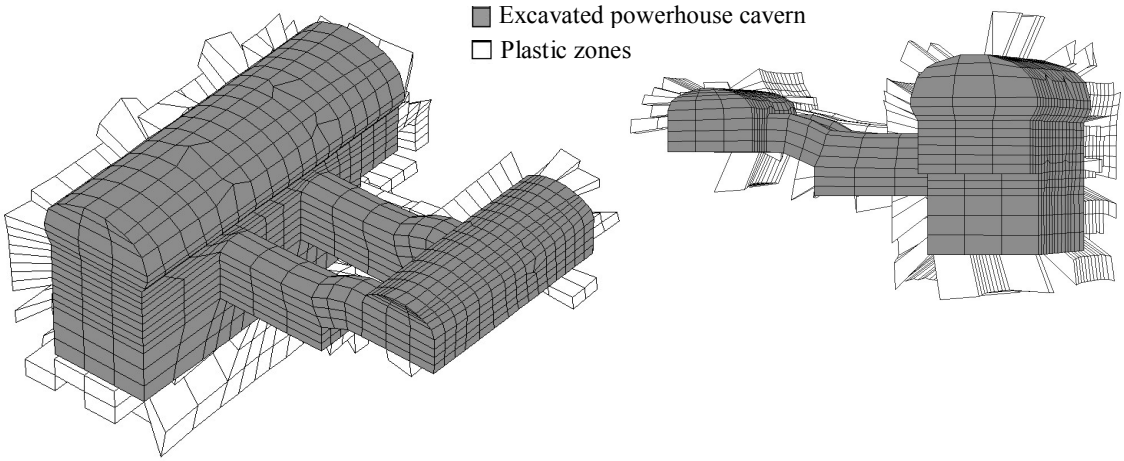

Figure 21. Plastic zones at the last excavation stage in the case of the second identification attempt.

4.2.2 *Identifications with the evolution strategies algorithm and comparisons between the two optimizations methods*

In order to verify that SiDoLo does not provide a local minimum, a probabilistic optimization method is performed in a second step. An evolution strategies algorithm is used to find the optimized values of the two parameters and obtained results are compared between the two methods. Only 18 displacements are used in the optimization process.

The computed displacements with the optimized values provided by the two methods are close to each other. Table 7 compares the parameters value provided by SiDoLo at the end of the second identification attempt to the values provided by the evolution strategies algorithm (ES), the respective error functions and the computation time required to achieve the identification process.

Table 7. Comparisons between the two optimization methods

Cases	E GPa	R -	Error function $\times 10^{-6}$	Time Hour
SiDoLo	56.7	1.90	1.34	14
ES	52.1	1.72	1.37	49
Difference	-8.1 %	-9.4 %	2.2 %	250 %

The error functions are quite similar. A difference of 8.1 % is observed on the Young modulus value provided by the two methods and for the in stresses ratio a difference of 9.4 % is obtained. The time required by the evolution strategies algorithm is more than 3 times higher in comparison with the time required for the other method. Only one generation is required in the evolution strategies algorithm to achieve the optimization process due to that for the parents of the first generation the stop criterion is verified. In order to verify that the solution provides by the evolution strategies algorithm corresponds to the global minimum it is necessary to decrease the tolerance criteria in order to obtain error function lower than 10^{-7} and to launch a new identification. But, the computation time will be important.

5 CONCLUSION

The use of inverse analysis on in situ measurements carried out during the construction of a real work is rare. This might be due to the difficulty met to apply inverse analysis (measurements quality, complexity of the geometry and of the excavation stages, …). In an underground works case, the numerical model required many simplifications in order to obtain acceptable computation times. The adopted constitutive model should not be too sophisticated with many parameters but should properly simulate the soil behaviour. For the studied cases, a linear elastic perfectly plastic model with a Mohr Coulomb failure criterion is considered to represent the soil mass.

This article shows the coupling of two optimization methods with 2D and 3D numerical modelling of two geotechnical works: a tunnel and underground powerhouse caverns.The use of a deterministic method may provide local minima. The probabilistic method based on evolution strategies permits to find global minimum. But this method required more important computation time. In the tunnel case, with two unknown parameters, the studied cost functions are not convex and present a valley. Moreover the error values are important for all the studied cost function (> 20 %). Thus the problem is difficult to solve. The solution found by the evolutionary algorithm varies according to the studied error function. For the second used function $L_E(A)$ it depends on the values of absolute and relative errors. But if just a relative error or an absolute error is considered the same solution is found. The solution changes according to the considered type of error. The calculation time is similar for all the error functions. This article shows also that the parent, combination and offspring population size influence the results. With an increase of the population size, the same error function value is obtained at the same number of generations. The provided value sets are different of about 10 % and the calculation time can increase of 50 %. In order to improve results a non linear elasticity and a Young modulus which varies with depth should be introduced. Moreover, maybe the evaluation of the earth pressure ratio by means of in situ tests needs to be more investigated. This ratio might be considered as a complementary parameter to identify.

In the complex powerhouse caverns case, a linear elastic constitutive model could be considered to represent the rock behaviour because a few plastic zones appear. And, this model should permit to reduce computation time. Moreover, in order to verify that the solution provides by the evolution strategies algorithm corresponds to the global minimum in the case of the complex powerhouse caverns, it is necessary to decrease the tolerance criteria and launch some new identifications.

AKNOWLEDGMENTS

The authors wish to express their acknowledge to Professor Lino Costa for providing the evolution strategy algorithm.

REFERENCES

Costa, L. & Oliveira, P. 2001. Evolutionary algorithms approach to the solution of mixed integer non linear programming problems. *Computers and Chemical Engineering* 25: 257-266.

Eclaircy-Caudron, S., Dias, D., Kastner, R. & Chantron, L. 2006. Identification des paramètres du sol rencontré lors du creusement d'un tunnel par analyse inverse. *Proc. JNGG 2006*. Lyon, France.

Finno, R.J. & Calvello, M. 2005. Supported Excavations: the Observational Method and Inverse Modeling. *Journal of Geotechnical and Geoenvironmental Engineering* 131(7): 826-836.

Goldberg, D. 1991. *Algorithmes génétiques : exploration, optimisation et apprentissage automatique.* Adisson-Wesley Edition.

Hicher, P.Y. & Shao, J.F. 2002. *Modèles de comportement des sols et des roches 2: lois incrémentales, viscoplasticité, endommagement*. Hermès Science Publications.

Itasca Consulting group 2005. *FLAC^{3D} user's manual*.

Itech 2002. *Cleo^{2D} user's manual*.

Jeon, Y.S. & Yang, H.S. 2004. Development of a back analysis algorithm using FLAC. *International Journal of Rock Mechanics and Mining Sciences* 41(1): 447-453.

Levasseur, S., Malecot, Y., Boulon, M. & Flavigny, E. 2005. Analyse inverse par algorithme génétique en géotechnique : application à un problème d'excavation. *17th Congrés Français de Mécanique*. Troyes, France.

Miranda, T., Gomes Correira, A., Ribeiro e Sousa, L. & Lima, C. 2005. Numerical modelling of a hydroelectric underground station using geomechanical parameters obtained by artificial intelligence techniques. *4th Portuguese-Mozambican of Engineering, Maputo,30 August-1 September 2005:807-816.*

Panet, M. 1995. *Le calcul des tunnels par la méthode convergence-confinement*. Presse de l'école nationale des Ponts et Chaussées.

Pilvin, P. 1983. Modélisation du comportement d'assemblages des structures à barres. *Ph. D. thesis*. Université Paris VI. Paris, France.

Renders, J.M. 1995. *Algorithmes génétiques et réseaux de neurones.* Hermès Science Publications.

Samarajiva, P. 2005. Genetic algorithms for the calibration of constitutive models for soils. *International Journal of Geomechanics*. *ASCE*. September 2005: 206-217.

Schwefel, H.-P. 1985. *Evolution and optimal seeking*. John Wiley and Sons.

SiDoLo version2.4495. 2003. *Notice d'utilisation*. Laboratoire Génie Mécanique et Matériaux de l'Université de Bretagne-Sud, Lorient.

Zentar, R. 1999. Analyse inverse des essais pressiométriques : Application à l'argile de Saint-Herblain. *Ph. D. thesis*. Ecole Centrale. Nantes, France.